

RSC Advances



This is an *Accepted Manuscript*, which has been through the Royal Society of Chemistry peer review process and has been accepted for publication.

Accepted Manuscripts are published online shortly after acceptance, before technical editing, formatting and proof reading. Using this free service, authors can make their results available to the community, in citable form, before we publish the edited article. This *Accepted Manuscript* will be replaced by the edited, formatted and paginated article as soon as this is available.

You can find more information about *Accepted Manuscripts* in the [Information for Authors](#).

Please note that technical editing may introduce minor changes to the text and/or graphics, which may alter content. The journal's standard [Terms & Conditions](#) and the [Ethical guidelines](#) still apply. In no event shall the Royal Society of Chemistry be held responsible for any errors or omissions in this *Accepted Manuscript* or any consequences arising from the use of any information it contains.



Journal Name

ARTICLE

Synthesis and characterization of CaFe_2O_4 catalyst for oleic acid esterification

Huei Ruey Ong,^a Md Maksudur Rahman Khan,^{a,*} Abu Yousuf,^b Nor Amalina Hussain,^a and Chin Kui Cheng^a

Received 00th January 20xx,
Accepted 00th January 20xx

DOI: 10.1039/x0xx00000x

www.rsc.org/

Esterification of free fatty acid (oleic acid) with ethanol over calcium ferrite catalyst was investigated in the present study. Calcium ferrite catalyst (CaFe_2O_4) was synthesized by the sol-gel method, which exhibited high catalytic activity for esterification of oleic acid. The morphology and size (500–1000 nm) of the synthesized catalyst were observed by scanning electron microscopy (SEM) and Energy-dispersive X-ray spectroscopy (EDS) was studied to ensure the absence of impurities. The orthorhombic structure of calcium ferrite was exposed by X-ray diffractometry (XRD). The effects of reaction variables such as catalyst loading, methanol to acid ratio, reaction time and temperature on the conversion of fatty acid were studied. The optimum condition for the esterification process was molar ratio of alcohol to oleic acid at 12:1 with 5 wt% of CaFe_2O_4 at 70°C with reaction time of 2 h. XRD patterns of recycled catalyst evidenced that catalyst structure was unchanged up to 3rd cycle, which indicated the long life of catalyst.

Introduction

Long chain methyl and ethyl esters derived from vegetable oil or animal fat, known as biodiesel, is considered as a potential alternative of diesel fuel. Theoretically, such oils and fats should not contain more than 1% free fatty acids (FFAs) since saponification of these FFAs reduces the yield of fatty acid alkyl esters (FAAEs) in alkaline transesterification reactions^{1–3}. Saponification is an undesirable reaction since it leads the extra cost for separation of biodiesel from glycerin and reduces the efficiency of the alkaline catalyst^{2,4}. Practically, higher levels of FFAs (up to 20%) were detected in waste oil, byproducts of the refining of vegetable oils, some nonedible oils, animal fats and oils that are presently used as a starting material for biodiesel production^{2,5,6}. To efficiently utilize these low-cost feedstocks for biodiesel synthesis, a preliminary acid-catalyzed esterification pretreatment is necessary to reduce their FFA contents⁷.

Although liquid acids such as H_2SO_4 , HF, H_3PO_4 and HCl are often used to lower the FFA level in those oils because of their high conversion and low cost, their usage are associated with effluent disposal problems, loss of catalyst and high equipment cost due to the corrosive nature of acids^{8–10}. The replacement of these hazardous and polluting corrosive homogeneous acid

catalysts by heterogeneous reusable catalysts is one of the major demands of the present society. Already a number of heterogeneous catalysts have been developed^{9,11,12}, but most of them are not practicable due to either low conversion efficiency or higher oil to alcohol molar ratio or short life time and requirements of high reaction time and temperature. Srilatha et al.⁹ used heteropoly tungstate supported on niobia catalysts at the conditions 25% of catalyst loading, 14:1 of methanol to palmitic acid molar ratio, 4 h of reaction time at 65°C and they achieved ~90% conversion of palmitic acid. Besides, tungstated zirconia⁷ was used to esterify lauric acid in a well-stirred semi-batch reactor at 130 °C at atmospheric pressure and 85% conversion was achieved by 2 h. Another solid acid catalyst ferric-alginate was studied by¹³ with 0.16:1 ferric-alginate to lauric acid mass ratio, 16:1 methanol to lauric acid molar ratio, 3 h and they obtained 97.7% methyl laurate. In the advanced level of solid acid catalyst study, attention has been focused on the porosity and particle size of the catalyst. Though Mekala et al.¹⁴ proposed a novel pore diffusion model where a major conversion of acidic acid occurs inside the catalyst pore, but the internal pore diffusion resistance was higher compared to bulk solution. Contrary, the large molecules have limited access to the internal pores of the catalyst pellets; hence the reaction occurs at the pore entrance, restricting further diffusion¹⁵. On the other hand, catalyst with high surface area can provide highest fatty acid methyl ester (FAME) yield¹⁶. Therefore, nano sized catalyst has become more attractive for the esterification of FFA. Wang et al.¹⁷ obtained ~96% conversion of waste cooking oil using aluminumdodecatungstophosphate (AIPW) nanotube as catalyst at 55°C, 1:34 oil/methanol ratio, 14 h of reaction time and 3 wt% of catalyst.

^a Faculty of Chemical and Natural Resources Engineering, Universiti Malaysia Pahang, 26300 Gambang Pahang, Malaysia.

^b Faculty of Engineering Technology, Universiti Malaysia Pahang, 26300 Gambang Pahang, Malaysia.

† Footnotes relating to the title and/or authors should appear here.

Electronic Supplementary Information (ESI) available: [details of any supplementary information available should be included here]. See DOI: 10.1039/x0xx00000x

Most of the esterification of FFA studies used methanol^{1,9} as a short chain alcohol, now a days ethanol has become more rational because of some advantages over methanol, propanol, butanol and some other larger chain alcohols¹⁸⁻²⁰. Ethanol can be derived from agricultural products and is renewable and biologically less objectionable in the environment¹⁸.

In the present work, we have studied the structural and morphological properties of calcium ferrite catalysts and analyzed its catalytic activities in order to ascertain its application in the biodiesel field.

Experimental section

Catalyst preparation

The catalyst was prepared by a sol-gel method. A stoichiometric ratio of $\text{Ca}(\text{NO}_3)_2 \cdot 4\text{H}_2\text{O}$ and $\text{Fe}(\text{NO}_3)_3 \cdot 9\text{H}_2\text{O}$ were mixed in a three-neck flask with 30 % aqueous NH_3 solution, and the mixture was stirred at 200 rpm and at room temperature for 24 h and sol was obtained^{21, 22}. The solution was then slowly heated to 80 °C and maintained at that temperature level until the water evaporated. The resulting brown dry gel-like slurry was calcined at 450 °C for 2 h followed by heat treatment at 1050 °C for 10 h using the furnace to obtain CaFe_2O_4 powder. Finally, CaFe_2O_4 powders were ground in the mortar. To recycle the catalyst, it was recovered by vacuum filtration unit using nylon membrane (pore size = 0.22 μm) followed by ethanol washing. The filter cake was dried in an oven at 100 °C, weighted and reused in the reaction system. Additionally, the method described by Oliveira et al., 2010 was followed to regenerate the catalyst, where after filtrating the catalyst was washed by n-hexane followed by drying in an oven at 100 °C. Finally the catalyst was calcined in a muffle furnace at 300 °C for 3 h.

Characterization of the catalyst

The acidity of the solid catalyst was determined by using Hammett indicator method. Acidic strength of the catalyst was tested using the modified method adopted from other studies^{13, 23}, where 0.1 g of dried catalyst was added to a test tube and suspended in 3–5 mL of anhydrous methanol. Then, one drop of 0.1% Hammett indicator (methyl violet, thymol blue, and methyl orange) was added and left to equilibrate for 2 h. Any changes in color were noted.

Nitrogen adsorption isotherms of the fresh catalyst and the used catalyst (after 3rd cycle) were measured at -196 °C using an ASAP 2010 apparatus (Micromeritics). Firstly, all samples were outgassed at room temperature then at 200 °C to a pressure of <0.2 Pa for 5 h. The specific surface area was determined by the Brunauer Emmett Teller (BET) method. The pore size distributions were measured by Barrett-Joyner-Halenda (BJH) method and the total pore volume was calculated from the amount of N_2 adsorbed up to $P/P_0 = 0.97$. X-ray diffraction patterns of the prepared catalyst were collected using X-ray diffractometer (Rigaku MiniFlex II) operated at accelerating voltage of 30 kV and emission current of 15 mA with graphite-monochromatized $\text{Cu-K}\alpha$ radiation and

scanning speed 1°/min. The scanning step size 0.02° was over a range of $2\theta = 20\text{--}80^\circ$.

X-ray photoelectron spectroscopy (XPS) analysis was carried out on a Quantum 2000 scanning ESCA microprobe system (Physical Electronics, Inc.). The microcrystalline structure and surface characteristics of the catalyst have been investigated by using Scanning Electron Microscope, SEM (Zeiss EVO MA 15). Sample powder was placed on an aluminum foil with double-sided carbon tape for energy dispersive x-ray spectroscopic (EDS) micro-analysis to determine the elemental compositions of the catalyst using JEOL JSM-7600, USA.

Esterification of Oleic acid with ethanol

The esterification reaction of oleic acid was performed in a 500 mL three necked round bottom flask and equipped with a reflux condenser. Oleic acid (50 mL) was added into the flask followed by a mixture of ethanol (18.5 – 166.5 mL) and CaFe_2O_4 catalyst of 1, 3, 5, 7 and 8 wt% to the weight of oleic acid. The molar ratio of ethanol to oleic acid was 2:1, 4:1, 6:1, 8:1, 12:1 and 18:1. The reaction temperature was followed as 40, 50, 60 and 70 °C. The reaction was initiated by stirring, typically at 250 rpm, and stopped after reaction time of 10 h for product analysis. The product solution was centrifuged and amount of FFA was determined by titration method (ASTM D5555). In brief, 4–5 g of samples were dispersed in isopropanol (75 mL) and hexane (15 mL) followed by titration against 0.25 N NaOH solution.

Characterization of spent catalysts

To reuse the catalyst, after the first cycle, it was recovered by simple filtration, washed with ethanol, dried in an oven at 100 °C, weighted and inserted in the reaction system again. To improve the activity of used catalyst, they were regenerated by calcination process. The recycled catalyst was washed a sequence with n-hexane, dried in an oven at 100°C and calcined at 300°C for 3 h, before the catalyst was placed in the reactor, the procedure was adopted from Oliveira et al.²⁴. XRD patterns of the reused catalyst were analyzed.

Results and Discussion

Catalyst characterization

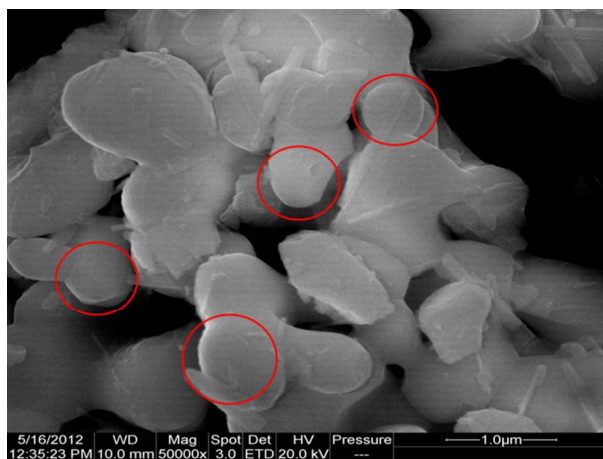
Catalyst acidity. The color change of indicators corresponding to their pH range which represent the acidity of the catalyst is presented in Table 1. The acid strength of the catalyst lies in the range between pH 1.6 and 2.8. This proves that the catalyst was strongly acidic and was most suitable for esterification reaction.

Table 1 Acidity of CaFe_2O_4 , determined by Hammett indicator method

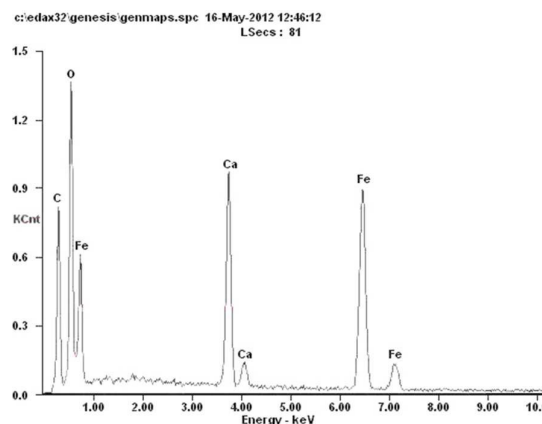
Indicators	Color change	pH range	Observed color (Fresh → after 3 rd cycle)
Methyl orange	Yellow → Red	3.2 – 4.4	Red (<3.2)
Thymol blue	Yellow → Red	1.2 – 2.8	Red (<1.2)
Methyl violet	Blue → Yellow	0.0 – 1.6	Blue

SEM and EDS analysis. SEM was used to exhibit the morphology and particle sizes of the samples. SEM images of calcined CaFe_2O_4 samples are shown in Fig. 1a. It can be observed that CaFe_2O_4 are nearly ball like spherical particles with the average diameter of 500 - 1000 nm. The particles are agglomerated form cluster structure and the sizes are relatively consisted with the broad size distribution, clearly represented in SEM analysis.

Crystallites of the CaFe_2O_4 samples could be consisted with the core-shell structure. The nonuniform crystalline core-shell structures of similar nanoparticles have recently been reported for MgFe_2O_4 , LiNbO_3 , NiFe_2O_4 ²⁵⁻²⁷. Meanwhile, the EDS spectrum, in Fig. 1b reveals that the CaFe_2O_4 spherical particles are mostly consisted with the higher purity of Ca, Fe, and O elements. In addition concentration and annealed temperature are significantly dominant to obtain the CaFe_2O_4 . The signal of O may be from contributions, first it is from the oxygen absorbed on the surface of the sample and second is from the sample itself.



(a)



(b)

Fig. 1 (a) SEM and (b) EDS of CaFe_2O_4 catalyst.

BET analysis

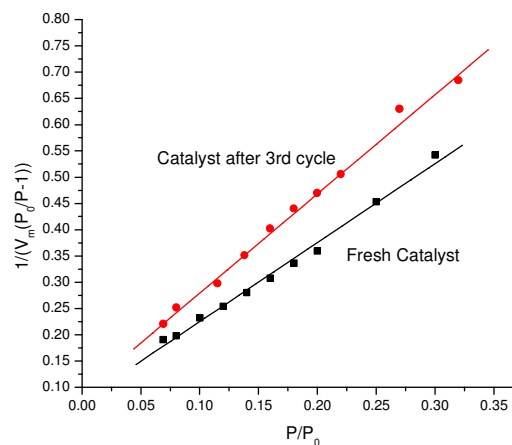


Fig. 2 Linearized BET plot for fresh CaFe_2O_4 and after 3rd cycle

The specific surface area of the catalyst was determined by the modelling of N_2 adsorption data with BET isotherm. The linearized BET plot is presented in Fig 2. The obtained BET surface area, average pore diameter and specific pore volume for the fresh catalyst, were $2.48 \text{ m}^2 \text{ g}^{-1}$, 96.11 \AA , and $0.0078 \text{ cm}^3 \text{ g}^{-1}$, respectively. The recycled catalyst after 3rd cycle showed the BET surface area, average pore diameter and specific pore volume as $1.97 \text{ m}^2 \text{ g}^{-1}$, 91.18 \AA , and $0.0063 \text{ cm}^3 \text{ g}^{-1}$, respectively. Around 20% decrease in the surface area in the recycled catalyst might be due to the blockage of the pores during the reaction and regeneration process.

XRD analysis. Crystalline structures of the CaFe_2O_4 particles could be clearly understood through the prominent use of XRD measurement. The sharp peaks from diffraction patterns show the crystalline nature of the samples. The XRD pattern of the

h. The maximum conversion (96%) was achieved by 4 h and there was no significant change with an extended time of reaction. Therefore, it would be very beneficial to replace the hazardous sulfuric acid catalyst by recyclable solid catalyst CaFe_2O_4 . Moreover, it showed better conversion efficiency under favourable conditions compared to other solid catalysts (Table 2).

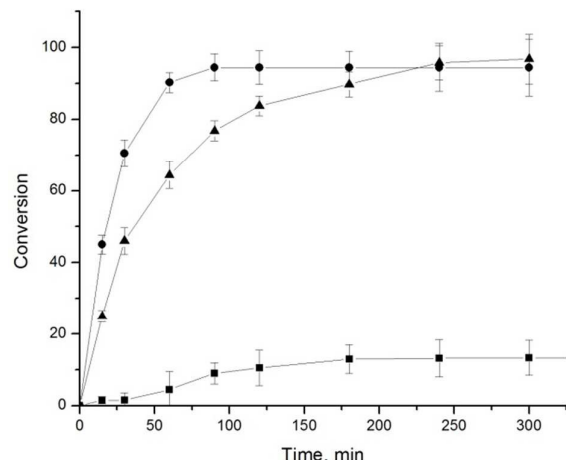


Fig. 5 Catalytic activity of CaFe_2O_4 solid catalyst, sulphuric acid and noncatalytic (reaction temperature, 70°C , mass amount of catalyst 5 wt%, ethanol/oleic acid mole ratio 12:1) ■ non-catalyzed ● H_2SO_4 catalyzed ▲ CaFe_2O_4 catalyzed.

Effect of catalyst concentration

Fig. 6 shows the effect of catalyst doses and it was examined by dosing 1, 3, 5, 7 and 8 wt% of CaFe_2O_4 to oleic acid maintaining the reaction temperature 70°C , ethanol/oleic acid mole ratio 12:1 and a reaction time 4 h. Using 1 wt% of catalyst, 70% conversion was achieved and the conversion ratio increased with the increasing catalyst amount, which could be attributed to the reason that more CaFe_2O_4 catalyst would provide more active reaction sites. It was clear that the amount of catalyst had a positive effect on the conversion ratio of oleic acid, and the conversion ratio (93%) became constant with catalyst amount above 5 wt%. Excess amount of catalyst may form emulsion which increased the viscosity and led to the formation of gels. The formation of emulsion will therefore block the reaction³⁵.

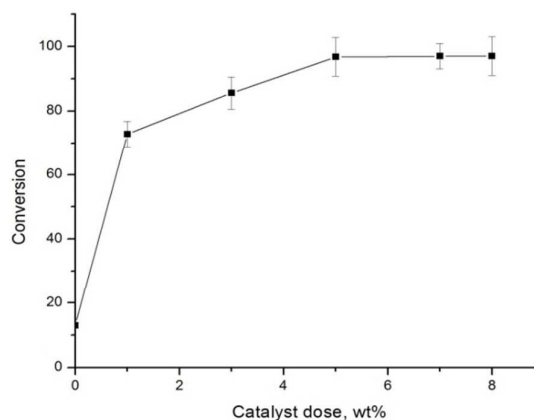


Fig. 6 Conversion of the oleic acid with diverse catalyst doses (reaction temperature, 70°C , ethanol/oleic acid mole ratio 12:1, reaction time 4 h).

Effect of ethanol/ oleic acid molar ratio

Fig. 7 shows the effect of various ethanol/oleic acid molar ratios (6:1, 12:1, 18:1) on the ethyl ester conversion at 5 wt% of CaFe_2O_4 catalyst and 70°C reaction temperature. As seen in Fig. 7, the ethyl ester conversion and the degree of the ethyl ester conversion depend largely upon ethanol/oleic acid molar ratio. The reaction was faster at the initial phase and reached a higher final conversion after 4 h and then it became constant. The conversion was increased from the ratio of 6:1 to 12:1 and it was unaffected for further increase to 18:1. The low yield at the feed ratio of 6:1 might be due to an insufficient quantity of ethanol for nucleophilic attack on the Brønsted acid sites of the catalyst¹¹. On the other hand, higher feed ratio did not increase the yield percentage and it might happen because of the production of water preferentially drives the hydrolysis of FAME into oleic acid³⁶.

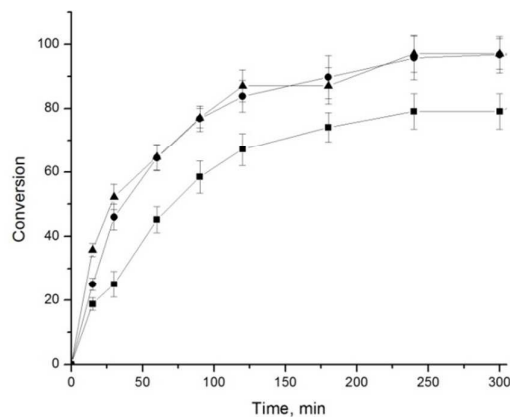


Fig. 7 Conversion of the oleic acid with diverse ethanol/oleic acid molar ratio (reaction temperature 70°C , mass amount of catalyst 5 wt%) ■ 6:1 ● 12:1 ▲ 18:1.

Effect of reaction temperature

The heterogeneous catalyzed esterification reaction is strongly influenced by the reaction temperature. The effect of the reaction temperature was studied from 40 to 70°C with ethanol/oleic acid molar ratio 12:1 and 5 wt. % of CaFe_2O_4 catalyst to oleic acid as shown in Fig. 8. The conversion rate of oleic acid was faster up to 1 h for all the batches, i.e., at 50°C, 60°C and 70°C. Subsequently, the conversion reached to the steady state. However, the conversion rate was increased with the increase of temperature and the value was 95% for 70°C. Fig. 8 also exhibits that the initial reaction rate was high, and then the reaction rate decreased. Fig 8 displays that the initial reaction rate was high for all temperature ranges followed by a decrease in reaction rate leading to a plateau. In the initial reaction periods, the reaction mixture was free from water, which subsequently produced as the reaction progressed causing the backward reaction to occur.³⁷

Initial reaction rate increased gradually with the increase of temperature (Table inside the Fig. 8). The reaction rate constant (k) for the esterification reaction of the oleic acid was determined by fitting the experimental data to the first-order reaction kinetic model. The rate constants were calculated as 0.0077, 0.0116, 0.0148 and 0.0178 s^{-1} for 40, 50, 60 and 70°C respectively. The activation energy was estimated as 24.60 kJ mole^{-1} from Arrhenius plot shown in the inset of Fig. 8. The smooth increase in rate constant with increase of temperature suggests that the mass transfer steps were not the rate limiting factor.

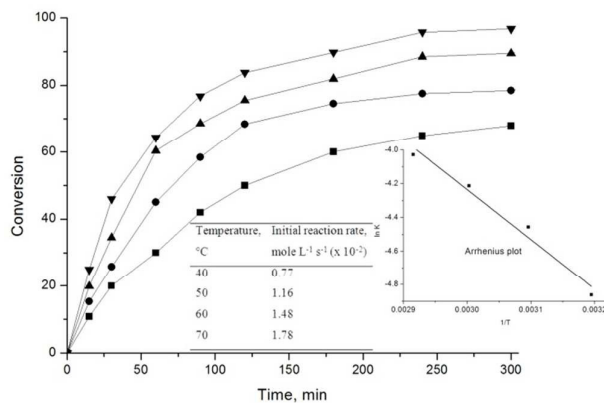


Fig. 8 Conversion of the oleic acid with diverse temperature on oleic acid conversion (mass concentration of catalyst 5 wt%, ethanol/oleic acid mole ratio 12:1) ■ 40°C ● 50°C ▲ 60°C ▼ 70°C, Inset the Figure: Arrhenius plot and Table of initial reaction rates.

Catalyst reactivation and recyclability

To recycle the catalyst, it was recovered by simple filtration, washed with ethanol, dried in an oven at 100 °C, weighted and inserted in the reaction system again. Fig. 9 shows the activity of the calcinated and uncalcinated catalysts during multi-cycle uses. Without calcination, the conversion drops from 96 to 76% after the first cycle and at the fourth cycle it was about 65% (Fig. 9: column Y). To improve the activity of used catalyst, they were regenerated by calcination process. A better performance was obtained with a sequence of washing with n-hexane, drying in an oven at 100°C and calcining at 300°C for 3 h²⁰. In this case, the conversion was improved 13% after the first cycle and about 9% after the second cycle, though the improvement was insignificant after the third cycle (Fig. 9: column X). On the other hand, XRD patterns (Fig. 3) indicated that the synthesized particles were mainly composed of CaFe_2O_4 . The fresh CaFe_2O_4 and used CaFe_2O_4 catalysts had well-crystallized structures with characteristic and symmetric reflections. Fresh CaFe_2O_4 and recycled CaFe_2O_4 (1st to 3rd cycles) catalysts had the same patterns, indicating that the CaFe_2O_4 catalyst was stable.

Journal Name

ARTICLE

Table 2 Esterification conditions of oleic acid by recently developed solid catalysts.

Acid catalyst	Temperature, °C	Reaction time, h	Alcohol: oleic acid	Catalyst doses, wt. %	Oleic acid conversion, %	Reference
1-butyl-3-methylimidazolium tetrachloroferrate ([BMIM][FeCl ₄])	65	3.6	22:1	-	83.4	4
H ₃ PW/ZrO ₂	100	4	6:1	20	88	20
Organophosphonic acid-functionalized silica SG-T-P	112	10	8.8:1	14.5	77.02	37
Sulfonated cation exchange resin	82	8	9:1	20g	93	38
Sulfonated carbons Starbons-300	80	3	10:1	1.33	60	39
CaFe ₂ O ₄	70	4	12:1	5	96	Present study

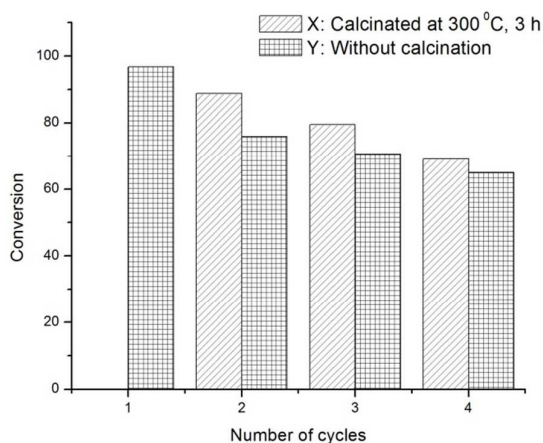


Fig. 9 Conversion of the oleic acid with recycled catalyst (reaction time 4h, mass concentration of catalyst 5wt%, ethanol/oleic acid mole ratio 12:1, reaction temperature 70°C).

Conclusions

The catalyst showed a remarkable success on the esterification of oleic acid with ethanol. The conversion of oleic acid reached equilibrium after an hour when all other reaction parameters were fixed. The maximum conversion of 96% was achieved under the conditions of ethanol to oil ratio 12:1, temperature 70°C and catalyst dose 5 wt%. Preliminary study of recyclability for CaFe₂O₄ indicated that a treatment of calcining at 300°C for 3 h recovered the conversion to about 88% and 80% after second and third cycles respectively. Further work is proceeding to increase its catalytic activity by impregnating precious metal to make the process industrially practicable.

Acknowledgements

Authors gratefully acknowledge the Faculty of Chemical and natural resources Engineering, University Malaysia Pahang for funding to carry out this work by a research grant (Project No.: RDU100395).

Notes and references

- M. Berrios, J. Siles, M. A. Martin and A. Martin, *Fuel*, 2007, **86**, 2383-2388.
- H. D. Hanh, N. T. Dong, K. Okitsu, R. Nishimura and Y. Maeda, *Renewable Energy*, 2009, **34**, 780-783.
- K.-S. Liu, *Journal of the American Oil Chemists' Society*, 1994, **71**, 1179-1187.
- A. H. M. Fauzi, N. A. S. Amin and R. Mat, *Appl. Energy.*, 2014, **114**, 809-818.
- S. V. Ghadge and H. Raheman, *Bioresour. Technol.*, 2006, **97**, 379-384.
- S. Zheng, M. Kates, M. A. Dubé and D. D. McLean, *Biomass Bioenerg.*, 2006, **30**, 267-272.
- K. Suwannakarn, E. Lotero, K. Ngaosuwan and J. G. Goodwin Jr, *Ind. Eng. Chem. Res.*, 2009, **48**, 2810-2818.
- F. Cao, Y. Chen, F. Zhai, J. Li, J. Wang, X. Wang, S. Wang and W. Zhu, *Biotechnol. Bioeng.*, 2008, **101**, 93-100.
- K. Srilatha, N. Lingaiah, B. L. A. P. Devi, R. B. N. Prasad, S. Venkateswar and P. S. S. Prasad, *Applied Catalysis A: General*, 2009, **365**, 28-33.
- Y. Zhang, M. A. Dube, D. D. I. McLean and M. Kates, *Bioresour. Technol.*, 2003, **89**, 1-16.
- K. U. Nandhini, B. Arabindoo, M. Palanichamy and V. Murugesan, *Journal of Molecular Catalysis A: Chemical*, 2006, **243**, 183-193.
- H. R. Ong, M. R. Khan, M. N. K. Chowdhury, A. Yousuf and C. K. Cheng, *Fuel*, 2014, **120**, 195-201.

13. B. Peng-Lim, S. Ganesan, G. P. Maniam and M. Khairuddean, *Energy*, 2012, **46**, 132-139.
14. M. Mekala, S. K. Thamida and V. R. Goli, *Chem. Eng. Sci.*, 2013, **104**, 565-573.
15. M. Absi-Halabi, A. Stanislaus, T. Al-Mughni, S. Khan and A. Qamra, *Fuel*, 1995, **74**, 1211-1215.
16. S. Yan, M. Kim, S. O. Salley and K. Y. S. Ng, *Appl. Catal. A Gen.*, 2009, **360**, 163-170.
17. J. Wang, Y. Chen, X. Wang and F. Cao, *BioResour.*, 2009, **4**, 1477-1486.
18. A. Demirbas, *Biomass and Bioenergy*, 2009, **33**, 113-118.
19. G. F. Ghesti, J. L. de Macedo, I. S. Resck, J. A. Dias and S. C. L. Dias, *Energy Fuels*, 2007, **21**, 2475-2480.
20. C. F. Oliveira, L. M. Dezaneti, F. A. C. Garcia, J. L. de Macedo, J. A. Dias, S. C. L. Dias and K. S. P. Alvim, *Appl. Catal. A Gen.*, 2010, **372**, 153-161.
21. B. Xin, P. Wang, D. Ding, J. Liu, Z. Ren and H. Fu, *Applied surface science*, 2008, **254**, 2569-2574.
22. J. Liqiang, S. Xiaojun, C. Weimin, X. Zili, D. Yaoguo and F. Honggang, *J. Phys. Chem. Solids*, 2003, **64**, 615-623.
23. P.-L. Boey, S. Ganesan, G. P. Maniam, M. Khairuddean and J. Efindi, *Energy Conversion and Management*, 2013, **65**, 392-396.
24. C. F. Oliveira, L. M. Dezaneti, F. A. Garcia, J. L. de Macedo, J. A. Dias, S. C. Dias and K. S. Alvim, *Applied Catalysis A: General*, 2010, **372**, 153-161.
25. H. U. Khan, I. Sterianou, S. Miao, J. Pokorny and I. M. Reaney, *Journal of Applied Physics*, 2012, **111**, 024107.
26. V. K. Mittal, S. Bera, T. Saravanan, S. Sumathi, R. Krishnan, S. Rangarajan, S. Velmurugan and S. V. Narasimhan, *Thin Solid Films*, 2009, **517**, 1672-1676.
27. V. Šepelák, I. Bergmann, A. Feldhoff, P. Heitjans, F. Krumeich, D. Menzel, F. J. Litterst, S. J. Campbell and K. D. Becker, *J. Phys. Chem. C*, 2007, **111**, 5026-5033.
28. Z. Liu, Z.-G. Zhao and M. Miyauchi, *J. Phys. Chem. C*, 2009, **113**, 17132-17137.
29. L. J. Berchmans, M. Myndyk, K. L. Da Silva, A. Feldhoff, J. Šubrt, P. Heitjans, K. D. Becker and V. Šepelák, *J. Alloy Compd.*, 2010, **500**, 68-73.
30. T. Yamashita and P. Hayes, *Appl. Surf. Sci.*, 2008, **254**, 2441-2449.
31. A. P. Grosvenor, B. A. Kobe, M. C. Biesinger and N. S. McIntyre, *Surface and Interface Analysis*, 2004, **36**, 1564-1574.
32. P. C. J. Graat and M. A. J. Somers, *Appl. Surf. Sci.*, 1996, **100**, 36-40.
33. S. J. Roosendaal, B. Van Asselen, J. W. Elsenaar, A. M. Vredenberg and F. H. P. M. Habraken, *Surface Science*, 1999, **442**, 329-337.
34. P. Zhang, Y. Gong, H. Li, Z. Chen and Y. Wang, *RSC Adv.*, 2013, **3**, 5121-5126.
35. L. Lin, D. Ying, S. Chaitep and S. Vittayapadung, *Applied Energy*, 2009, **86**, 681-688.
36. S. Gan, H. K. Ng, P. H. Chan and F. L. Leong, *Fuel Processing Technology*, 2012, **102**, 67-72.
37. P. Yin, L. Chen, Z. Wang, R. Qu, X. Liu and S. Ren, *Bioresource technology*, 2012, **110**, 258-263.
38. Y. Jiang, J. Lu, K. Sun, L. Ma and J. Ding, *Energy Conversion and Management*, 2013, **76**, 980-985.
39. A. Aldana-Pérez, L. Lartundo-Rojas, R. Gómez and M. E. Niño-Gómez, *Fuel*, 2012, **100**, 128-138.